

The lowest ${}^2A'$ excited state of the water-hydroxyl complex

T. Daniel Crawford^{a)} and Micah L. Abrams
Department of Chemistry, Virginia Tech, Blacksburg, Virginia 24061

Rollin A. King
Department of Chemistry, Bethel University, St. Paul, Minnesota 55112

Joseph R. Lane, Daniel P. Schofield,^{b)} and Henrik G. Kjaergaard^{c)}
Department of Chemistry, University of Otago, P.O. Box 56, Dunedin 9054, New Zealand

(Received 20 September 2006; accepted 12 October 2006; published online 22 November 2006)

Vertical and adiabatic excitation energies of the lowest ${}^2A'$ excited state in the water-hydroxyl complex have been determined using coupled cluster, multireference configuration interaction, multireference perturbation theory, and density-functional methods. A significant redshift of about 0.4 eV in the vertical excitation energy of the complex compared to that of the hydroxyl radical monomer is found with the coupled cluster calculations validating previous results. Electronic excitation leads to a structure with near-equal sharing of the hydroxyl hydrogen by both oxygen atoms and a concomitantly large redshift of the adiabatic excitation energy of approximately 1 eV relative to the vertical excitation energy. The combination of redshifts ensures that the electronic transition in the complex lies well outside the equivalent excitation in the hydroxyl radical monomer. The complex is approximately five times more strongly bound in the excited state than in the ground state. © 2006 American Institute of Physics. [DOI: 10.1063/1.2388260]

I. INTRODUCTION

The hydroxyl radical (OH) is one of the most important reactive intermediates and the primary oxidant in the troposphere. The hydroxyl radical forms hydrogen bonded complexes with water, which are expected to change the physical and chemical properties of OH and hence may also be of importance in the atmosphere.¹⁻⁴ The complex was first detected in matrix isolation experiments, and the resulting infrared spectrum agreed well with *ab initio* calculated frequencies of the $H_2O \cdot HO$ structure in which the hydroxyl hydrogen atom is involved in the hydrogen bond.⁵⁻⁷

The lowest excited state of the complex is of ${}^2A''$ symmetry and arises from the splitting of the degenerate ${}^2\Pi$ ground state of the hydroxyl radical monomer in the presence of a water molecule. Early *ab initio* studies of $H_2O \cdot HO$ focused on the ground state and the ${}^2A''$ excited state.^{8,9} Very recently, the rotational spectrum of the complex was recorded,^{10,11} and the microwave study of Brauer *et al.* found this excited state to lie approximately 200 cm^{-1} above the ground ${}^2A'$ state,¹¹ in agreement with theoretical estimates.¹²

Measurements of the atmospheric concentration of the OH radical often use a rotationally resolved line in the ${}^2\Sigma^+ \leftarrow {}^2\Pi$ electronic transition lying in the UV at about 308 nm (4 eV).¹³ In the $H_2O \cdot HO$ complex, this transition corresponds to ${}^2A' \leftarrow {}^2A'$, for which Schofield and Kjaergaard recently reported multireference configuration interac-

tion (MRCI) and Davidson-corrected MRCI (MRCI+Q) calculations.³ The MRCI vertical excitation energies were found to lie approximately 0.3 eV to the red of the corresponding ${}^2\Sigma^+ \leftarrow {}^2\Pi$ excitation of the hydroxyl radical monomer. Hence, hydroxyl radicals that form complexes with water molecules are unlikely to be accounted for in atmospheric measurements. It was suggested that the redshifted ${}^2A' \leftarrow {}^2A'$ transition could be used to identify the complex in the gas phase and in the atmosphere.³ However, the MRCI method is not size extensive, which could lead to errors in the predicted shifts.

This paper expands upon the earlier work of Schofield and Kjaergaard in two ways.³ First, we examine the significance of the change in geometric structure upon electronic excitation in the $H_2O \cdot HO$ complex, i.e., the adiabatic excitation. Second, we make use of both coupled cluster and multiconfigurational perturbation theory excitation energy methods in order to test the reliability of the MRCI method. In particular, we apply the equation-of-motion coupled cluster singles and double (EOM-CCSD) model¹⁴ as well as the recently developed open-shell CC3 linear-response approach,¹⁵ both of which are size extensive and considered to be among the most accurate methods currently available for excited states dominated by a single excitation relative to the reference state. In addition, we apply the complete active space self-consistent field plus second-order perturbation theory (CASPT2) approach of Roos and co-workers¹⁶⁻¹⁸ for additional consideration of potential multireference effects.

II. COMPUTATIONAL METHODS

Properties of the ground and excited states of the $H_2O \cdot HO$ complex have been determined using coupled clus-

^{a)}Electronic mail: crawdad@vt.edu

^{b)}Current address: Center for Molecular and Materials Simulations, Department of Chemistry, University of Pittsburgh, Pittsburgh, PA 15260.

^{c)}Currently on leave at the Lundbeck Foundation Center for Theoretical Chemistry, Department of Chemistry, Aarhus University, DK-8000 Aarhus C, Denmark.

TABLE I. Optimized geometry of the ground ${}^2A'$ electronic state of the $\text{H}_2\text{O}\cdot\text{HO}$ complex. Bond lengths are given in Angstroms and bond angles in degrees, which are computed using the aug-cc-pVTZ basis set.

Parameter	CCSD(T)	MRCI	CASPT2	B3LYP
$r_{\text{O}_1\text{H}_1}$	0.9747	0.9691	0.9840	0.9838
$r_{\text{H}_1\text{O}_1}$	1.8934	1.9418	1.8996	1.8959
$r_{\text{O}_2\text{H}_2}$	0.9594	0.9613	0.9629	0.9624
$r_{\text{O}_1\text{O}_2}$	2.8679	2.9089	2.8823	2.8791
$\theta_{\text{O}_1\text{H}_1\text{O}_2}$	178.9	177.6	176.0	177.6
$\theta_{\text{H}_1\text{O}_2\text{H}_2}$	119.8	119.2	116.5	119.3
$\tau_{\text{O}_1\text{H}_1\text{O}_2\text{H}_2}$	66.3	64.9	62.2	66.3
$\tau_{\text{O}_1\text{O}_2\text{H}_3\text{H}_2}$	138.2	136.1	130.1	137.2

ter (CC),¹⁹ MRCI,²⁰ CASPT2,¹⁶ and time-dependent density-functional^{21–23} methods in conjunction with the augmented correlation-consistent triple-zeta (aug-cc-pVTZ) basis set of Dunning and co-workers.^{24,25}

Electronic excitation energies and oscillator strengths were obtained using the EOM-CCSD method¹⁴ and excitation energies only using the open-shell CC3 method,¹⁵ both with spin-restricted open-shell Hartree-Fock (ROHF) reference wave functions. Spin-unrestricted [UHF] reference wave functions give CCSD and CC3 excitation energies to within 0.01 eV of their ROHF counterparts in all cases and are thus not reported.

Multireference calculations of these same properties were carried out using a state-averaged complete active space self-consistent field (CASSCF) reference function based on the lowest two ${}^2A'$ states as well as the lowest ${}^2A''$ state. All CASSCF calculations were based on a full valence active space (15 electrons in 11 orbitals), and the $1s$ core orbitals remained unoptimized. Subsequent MRCI and CASPT2 calculations were carried out using only those CASSCF configurations with coefficients ≥ 0.001 based on previous calculations.²⁶ In all MRCI and CASPT2 ground- and excited-state calculations, both of the lowest ${}^2A'$ states were computed simultaneously to allow for a consistent comparison between wave functions for each state.

EOM-CCSD and CC3 vertical excitation energy calculations were carried out at the CCSD(T)/aug-cc-pVTZ^{27,28} optimized geometry of the $\text{H}_2\text{O}\cdot\text{HO}$ complex. MRCI, CASPT2, and B3LYP^{29,30} vertical excitation energies were computed at the optimized structures at the corresponding levels of theory. Optimized structures were obtained using analytic energy gradients with the CCSD(T)^{31,32} and B3LYP methods and using finite differences of energies with the MRCI and CASPT2 methods. Adiabatic excitation energies, T_e , were obtained by taking the difference in energies of the optimized structures of ground and excited states. The excited-state structure was optimized at the EOM-CCSD³³ and B3LYP levels of theory using analytic energy gradients and at the MRCI and CASPT2 levels of theory using finite differences of energies. Oscillator strengths were computed with the formula given in Ref. 3 using transition moments and energies taken from the respective *ab initio* or density-functional calculations. Harmonic vibrational frequency calculations were carried out using finite differences of analytic

TABLE II. Optimized geometry of the lowest excited ${}^2A'$ electronic state of the $\text{H}_2\text{O}\cdot\text{HO}$ complex. Bond lengths are given in Angstroms and bond angles in degrees, which are computed using the aug-cc-pVTZ basis set.

Parameter	EOM-CCSD	MRCI	CASPT2	B3LYP
$r_{\text{O}_1\text{H}_1}$	1.1536	1.1656	1.1692	1.1200
$r_{\text{H}_1\text{O}_2}$	1.1667	1.1686	1.1614	1.2389
$r_{\text{O}_2\text{H}_2}$	0.9648	0.9693	0.9715	0.9707
$r_{\text{O}_1\text{O}_2}$	2.3120	2.3241	2.3192	2.3491
$\theta_{\text{O}_1\text{H}_1\text{O}_2}$	170.3	169.3	168.7	169.5
$\theta_{\text{H}_1\text{O}_2\text{H}_2}$	102.5	101.7	101.2	100.6
$\tau_{\text{O}_1\text{H}_1\text{O}_2\text{H}_2}$	55.3	54.7	54.6	54.9
$\tau_{\text{O}_1\text{O}_2\text{H}_3\text{H}_2}$	103.4	101.6	100.7	100.5

energy gradients at the CCSD(T) and EOM-CCSD levels of theory.

All EOM-CCSD and CC3 vertical excitation energy and oscillator strength calculations were performed with the PSI3 program package,³⁴ and all coupled cluster structural optimizations and vibrational analyses with the ACES2 package.³⁵ Coupled cluster structural optimizations and vibrational analyses were carried out with all electrons correlated, while all vertical and adiabatic single-point energies held the oxygen $1s$ core orbitals frozen. All MRCI and CASPT2 calculations were carried out using the MOLPRO quantum chemistry package.³⁶ Density-functional calculations of these properties were carried out using the Becke three-parameter exchange functional²⁹ in combination with the Lee-Yang-Parr correlation functional,³⁰ as implemented in the TURBOMOLE program package.³⁷

III. RESULTS AND DISCUSSION

A. Structures

Tables I and II report the ground- and excited-state geometries of the water-hydroxyl complex at several levels of theory. Figure 1 depicts the structures and defines the atom ordering used in the tables. The ground-state structure agrees well with that reported earlier by Schofield and Kjaergaard at the QCISD/6-311++G(2d,2p) level of theory,³ the coupled

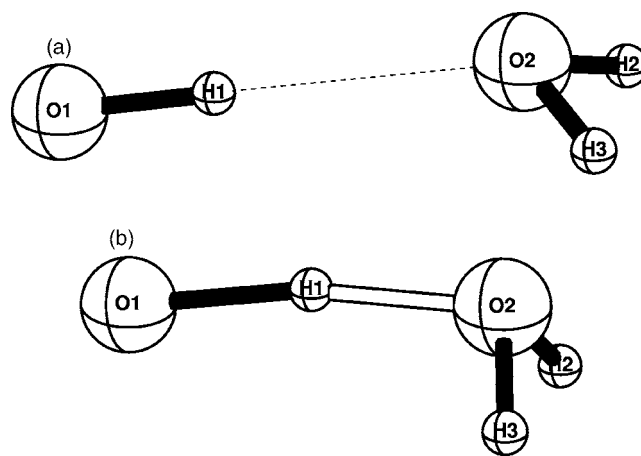


FIG. 1. Optimized geometries of the ${}^2A'$ ground and lowest-lying excited ${}^2A'$ state of the $\text{H}_2\text{O}\cdot\text{HO}$ complex.

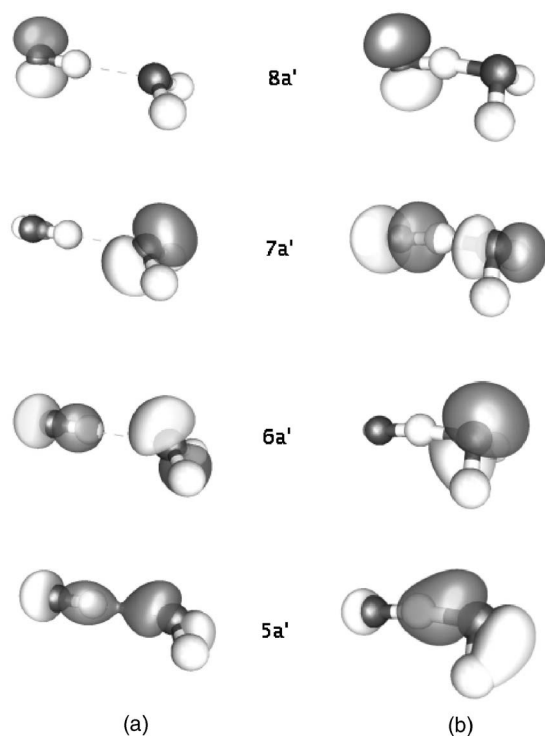


FIG. 2. Selected Hartree-Fock molecular orbitals of the ${}^2A'$ ground state of $\text{H}_2\text{O}\cdot\text{HO}$ at the (a) ground- and (b) excited-state optimized structures.

cluster results of Ohshima *et al.*¹⁰ and of Du *et al.*,³⁸ and the earlier configuration interaction (CI) studies of Schaefer and co-workers.^{8,9} All of the high-level *ab initio* and density-functional methods used here agree well on the structure of each state. In addition, the CCSD(T)/aug-cc-pVTZ ground-state structure in Table I has a $(B+C)/2$ averaged rotational constant of 6856.3 MHz, which differs from that derived from experimental microwave data recently reported by Brauer *et al.* by approximately 4%.¹¹ The CCSD(T) calculated $\text{H}_1\text{-O}_2$ distance of 1.893 Å is also in reasonable agreement with the experimentally inferred (vibrationally averaged) distance of 1.952 Å.

On the other hand, the ground- and excited-state structures differ from each other in three significant ways: (1) the hydroxyl hydrogen atom lies nearly equidistant between the two oxygen atoms in the excited state, whereas in the ground state it is primarily associated with the hydroxyl oxygen; (2) the angle between the O–O axis and the plane of the water molecule is just over 100° in the excited state, while in the ground state the angle is much wider at approximately 135° ; and (3) the O–O distance is shortened by more than 0.5 Å, indicating a much more strongly bound complex in the excited state.

We have calculated Hartree-Fock molecular orbitals (MOs) at the ground- and excited-state geometries to investigate the structural differences arising upon the ${}^2A' \leftarrow {}^2A'$ excitation. Selected MOs of a' symmetry are shown in Fig. 2. In both the ground- and excited-state geometries, the singly occupied $8a'$ orbital consists primarily of a p -type orbital on the hydroxyl oxygen atom in the symmetry plane of the complex. At the ground-state geometry, the highest doubly occupied $7a'$ orbital is essentially the oxygen lone pair lying

out of the plane of the water molecule, with a small contribution of opposite sign from the hydroxyl-oxygen lone pair lying along the O–H bond axis. This orbital combination results in a slight antibonding character between the oxygen atom of the water molecule and the hydrogen atom of the hydroxyl radical. Similarly, the second- and third-highest doubly occupied a' orbitals ($6a'$ and $5a'$) can be described, respectively, as negative and positive combinations of the oxygen lone pair lying in the plane of the water and the hydroxyl-oxygen lone pair lying along the O–H bond axis.

In the excited-state geometry, the above MO picture changes somewhat. While the highest doubly occupied $7a'$ orbital is similar to its ground-state counterpart in that it exhibits a significant contribution from the oxygen lone pair lying out of the plane of the water molecule, the contribution from the hydroxyl-oxygen lone pair along the O–H bond axis is significantly larger than in the ground-state geometry. Furthermore, given that these two atomic orbitals (AOs) contribute to the $7a'$ MO with opposite signs, the near perpendicularity between the plane of the water molecule and the O–H–O axis at this geometry (cf. Fig. 1) appears to result in increased antibonding character between the oxygen of the water and the hydrogen of the hydroxyl.

One possible explanation for the large difference between the ground- and excited-state structures may be found by considering the differences in the key MOs involved in the excitation. At the ground-state geometry, the lowest ${}^2A'$ excited-state arises primarily from single excitations into the singly occupied orbital from the three highest-energy doubly occupied a' MOs with respective EOM-CCSD excitation coefficients of 0.35 ($7a' \rightarrow 8a'$), 0.70 ($6a' \rightarrow 8a'$), and 0.58 ($5a' \rightarrow 8a'$). However, at the optimized geometry of the excited state, the transition is completely dominated (with a coefficient of 0.96) by the single excitation from the highest a' doubly occupied orbital ($7a'$) into the singly occupied orbital ($8a'$). This highest doubly occupied $7a'$ orbital exhibits much greater antibonding character between the oxygen atom of the water molecule and the hydrogen atom of the hydroxyl radical than the $5a'$ and $6a'$ orbitals or their counterparts at the ground-state geometry. Thus, the excitation serves to reduce the apparent antibonding character of the many-electron state and reduces the distance between the molecular fragments. In addition, the lack of excitation out of the $5a'$ MO, which is bonding between the hydroxyl-hydrogen and the water-oxygen, provides greater energetic stabilization at the excited-state geometry.

The calculated harmonic vibrational frequencies of the ground and excited states are given in Table III. The values reported for the ground state are typical of weak hydrogen bonded complexes^{39,40} and are in agreement with previous calculations.^{7,9} Table III shows the characteristic HOH-bending and OH-stretching frequencies with the hydroxyl OH stretch (ω_2) redshifted due to its involvement in the hydrogen bond.⁷ In addition, five low frequency modes involve intermolecular vibrations. In the excited state these characteristic low-frequency vibrations shift to significantly higher frequencies because of a significant increase in binding between the OH and H_2O moieties, as is evident in the large reduction of the O–O distance. The bending and stretching

TABLE III. Coupled cluster harmonic vibrational frequencies (in cm^{-1}) and infrared integrated absorption intensities (in km/mol in parentheses) for the ground state and first excited ${}^2A'$ state of the $\text{H}_2\text{O}\cdot\text{HO}$ complex (computed using the aug-cc-pVTZ basis set).

Mode	Ground state CCSD(T)	Excited state EOM-CCSD	Mode description
$\omega_1(a')$	3836.2(9.9)	3791.2(77.1)	H_2O symmetric stretch
$\omega_2(a')$	3645.1(296.7)	1930.1(2087.5)	OH stretch
$\omega_3(a')$	1643.0(71.0)	1666.1(57.5)	H_2O bend
$\omega_4(a')$	462.4(151.7)	1406.3(204.3)	O–H–O in-plane bend
$\omega_5(a')$	193.8(26.5)	696.6(46.2)	O–O stretch
$\omega_6(a')$	152.7(167.2)	471.0(167.2)	H_2O wag
$\omega_7(a'')$	3939.1(82.6)	3873.2(153.3)	H_2O asymmetric stretch
$\omega_8(a'')$	556.2(141.5)	1475.9(37.7)	O–H–O out-of-plane bend
$\omega_9(a'')$	233.2(3.4)	406.9(13.3)	H_2O twist

frequencies of the water molecule are maintained in the excited state, but the near-equal sharing of the hydroxyl hydrogen between the two oxygen atoms (cf. Fig. 1 and Table II) reduces the hydroxyl stretching vibrational frequency to 1930 cm^{-1} , much lower than a typical OH stretching frequency, and increases its integrated absorption intensity by nearly an order of magnitude. The hydroxyl in-plane (ω_4) and out-of-plane (ω_8) bending frequencies increase significantly in the excited state to values typical for O–H–O bending modes. In some anionic complexes, where the O–O distance is similar to that in the $\text{H}_2\text{O}\cdot\text{HO}$ excited state, similar frequencies are observed for the comparable vibrational modes.⁴¹ It is perhaps more reasonable to consider the excited state as a molecule held together by weak covalent bonds rather than a complex.

B. Electronic transitions

Table IV reports vertical excitation energies and oscillator strengths, as well as adiabatic excitation energies of the lowest ${}^2A' \leftarrow {}^2A'$ transition in the $\text{H}_2\text{O}\cdot\text{HO}$ complex. Table V reports the corresponding data for the ${}^2\Sigma^+ \leftarrow {}^2\Pi$ transition in the hydroxyl radical. The present MRCI vertical excitation energies and oscillator strengths compare closely with those from Ref. 3. The CCSD and CC3 methods give very similar results with the vertical excitation energy differing by less than 0.01 eV for both OH and the complex. Slightly more variation is seen in the adiabatic excitation energies.

Both the vertical and adiabatic excitation energies predicted by each level of theory are very consistent—varying by 0.17 eV at most among the wave-function-based ap-

TABLE IV. Vertical and adiabatic excitation energies (in eV) and oscillator strengths $\times 10^3$ (unitless) of the lowest ${}^2A' \leftarrow {}^2A'$ transition of the $\text{H}_2\text{O}\cdot\text{HO}$ complex (computed using the aug-cc-pVTZ basis set).

Method	Vertical	Adiabatic (T_e)	Oscillator strength
CCSD	3.77	2.88	1.75
CC3	3.76	2.80	...
MRCI	3.87	2.94	1.77
MRCI+ Q	3.82	2.85	...
CASPT2	3.74	2.77	1.36
B3LYP	3.62	2.79	1.61

TABLE V. Vertical and adiabatic excitation energies (in eV) and oscillator strengths $\times 10^3$ (unitless) for the lowest ${}^2\Sigma^+ \leftarrow {}^2\Pi$ transition in the hydroxyl radical (computed using the aug-cc-pVTZ basis set).

Method	Vertical	Adiabatic	Oscillator strength
CCSD	4.13	4.09	1.55
CC3	4.13	4.09	...
MRCI	4.18	4.14	1.71
MRCI+ Q	4.12	4.08	...
CASPT2	4.18	4.15	1.66
B3LYP	4.21	4.17	1.41

proaches and with the B3LYP vertical excitation energies somewhat lower. This result, along with the methods' corresponding consistency in the structural predictions, suggests that the excitation energies have a high degree of reliability. We also note that the close comparison between the MRCI and CASPT2 versus coupled cluster results as well as the small CCSD T_1 diagnostic⁴² (approximately 0.009) and maximum T_2 amplitude (approximately 0.02) indicate that the electronic states in question exhibit little to no multiconfigurational character.

Previous MRCI calculations found a substantial redshift in the ${}^2\Sigma^+ \leftarrow {}^2\Pi$ vertical excitation energy of OH upon formation of the complex.³ The present coupled cluster calculations predict a slightly larger shift of 0.37 eV, suggesting that the non-size-extensive MRCI method gives reasonable results for a complex of this limited size. The increase in vertical excitation energy shifts the electronic absorption band of the complex even further away from the OH transitions. Although 0.07 eV is a relatively small error in an *ab initio* calculation of an electronic excitation, it corresponds to about 5 nm (or 600 cm^{-1}) at these transition energies, which is substantial in spectroscopic detection and atmospheric simulations. The CCSD oscillator strength of the ${}^2\Sigma^+ \leftarrow {}^2\Pi$ transition in OH of 1.55×10^{-3} is close to the experimental oscillator strength of 1.3×10^{-3} (see Ref. 43).

We find a large redshift of 0.96 eV (CC3/aug-cc-pVTZ) in the adiabatic excitation energies relative to the vertical energies, a result that is to be expected, given the large geometry and electronic structure changes between the ground and excited states. The combination of the difference in vertical and adiabatic excitation energies from the ${}^2A' \leftarrow {}^2A'$ transition and the 0.37 eV redshift (CC3) arising from the formation of the complex clearly indicates a substantial perturbation of the UV absorption spectrum relative to that of the OH radical monomer.

In the ground state, the binding energy of the water-hydroxyl radical complex is approximately 6.4 kcal/mol at the CCSD(T)/aug-cc-pVTZ level of theory (not including counterpoise or zero-point vibrational corrections). At the same level of theory, the binding energy of the water dimer is 5.2 kcal/mol, and the structures of the two complexes are similar. If we assume that the excited state of $\text{H}_2\text{O}\cdot\text{HO}$ dissociates to OH in its ${}^2\Pi$ excited state and H_2O in its ground state, we find a dissociation energy of 34.3 kcal/mol (1.49 eV) at the EOM-CCSD/aug-cc-pVTZ level of theory. Thus, the excited state is much more strongly bound than the ground state.

The large difference in vertical and adiabatic excitation energies suggests that the electronic excitation spectrum of $\text{H}_2\text{O}\cdot\text{HO}$ will consist of a long vibrational progression. We find that the combination of the adiabatic excitation energy and the dissociation energy of the excited state (4.3 eV) is larger than the vertical excitation energy (3.8 eV). Thus, the absorption spectrum of the complex should be observable, but its structure may be broad and featureless.

IV. CONCLUSIONS

We have optimized the structure of the water-hydroxyl complex in the ground and excited ${}^2A'$ states and calculated the corresponding vertical and adiabatic excitation energies using coupled cluster, multireference configuration interaction, multireference perturbation theory, and density-functional methods.

With the CC3/aug-cc-pVTZ method, we find a significant redshift of 0.37 eV in the vertical excitation energy of the water-hydroxyl complex compared to that of the equivalent ${}^2\Sigma^+ \leftarrow {}^2\Pi$ transition in the hydroxyl radical monomer corroborating previous MRCI results.

The structure of the $\text{H}_2\text{O}\cdot\text{HO}$ complex is found to change significantly on excitation to the first ${}^2A'$ excited state. The distance between the two oxygen atoms is reduced by more than 0.5 Å, resulting in a near-equal sharing of the hydroxyl hydrogen by both oxygen atoms. In addition, a concomitantly large reduction in the angle between the O–O axis relative to the plane of the water molecule appears to contribute to the greater stability of the complex in the excited state. We find that the complex is significantly more strongly bound in the excited state than in the ground state to such an extent that $\text{H}_2\text{O}\cdot\text{HO}$ in the first ${}^2A'$ excited state is perhaps better thought of as a covalently bound molecule than a weakly bound complex. This is supported by changes in the calculated harmonic frequencies between the ground and excited states.

These significant structural changes between the ground and excited ${}^2A'$ states lead to a large red-shift of the adiabatic excitation energy of just under 1.0 eV relative to the vertical excitation energy. This redshift and the stronger binding in the excited state suggests that the ${}^2A' \leftarrow {}^2A'$ UV absorption in $\text{H}_2\text{O}\cdot\text{HO}$ will be broad and featureless. The significant shift from the electronic transitions in OH will make this electronic transition suitable for the detection of the complex and the determination of its atmospheric concentration.

ACKNOWLEDGMENTS

The authors thank Poul Jørgensen for helpful discussions. This work was supported by a National Science Foundation CAREER award (CHE-0133174), a Cottrell Scholar Award from the Research Corporation, the Marsden Fund administered by the Royal Society of New Zealand, and the University of Minnesota Supercomputing Institute. One of the authors (J.R.L.) is grateful to the Foundation for Research, Science and Technology for a Bright Futures scholarship. Another author (H.G.K.) is grateful to the Research Foundation at Aarhus University for a visiting professorship.

- ¹S. Aloisio and J. S. Francisco, *Acc. Chem. Res.* **33**, 825 (2000).
- ²V. Vaida, H. G. Kjaergaard, and K. J. Feierabend, *Int. Rev. Phys. Chem.* **22**, 203 (2003).
- ³D. P. Schofield and H. G. Kjaergaard, *J. Chem. Phys.* **120**, 6930 (2004).
- ⁴V. Vaida, *Int. J. Photoenergy* **7**, 61 (2005).
- ⁵A. Engdahl, G. Karlström, and B. Nelander, *J. Chem. Phys.* **118**, 7797 (2003).
- ⁶V. S. Langford, A. J. McKinley, and T. I. Quickenden, *J. Am. Chem. Soc.* **122**, 12859 (2000).
- ⁷P. D. Cooper, H. G. Kjaergaard, V. S. Langford, A. J. McKinley, T. I. Quickenden, and D. P. Schofield, *J. Am. Chem. Soc.* **125**, 6048 (2003).
- ⁸K. S. Kim, H. S. Kim, J. H. Jang, H. S. Kim, B.-J. Mhin, Y. Xie, and H. F. Schaefer, *J. Chem. Phys.* **94**, 2057 (1991).
- ⁹Y. Xie and H. F. Schaefer, *J. Chem. Phys.* **98**, 8829 (1993).
- ¹⁰Y. Ohshima, K. Sato, Y. Sumiyoshi, and Y. Endo, *J. Am. Chem. Soc.* **127**, 1108 (2005).
- ¹¹C. S. Brauer, G. Sedo, E. M. Grumstrup, K. R. Leopold, M. D. Marshall, and H. O. Leung, *Chem. Phys. Lett.* **401**, 420 (2005).
- ¹²M. D. Marshall and M. I. Lester, *J. Phys. Chem. B* **109**, 8400 (2005).
- ¹³T. Brauers, M. Hausmann, A. Bister, A. Kraus, and H.-P. Dorn, *J. Geophys. Res.* **106**, 7399 (2001).
- ¹⁴J. F. Stanton and R. J. Bartlett, *J. Chem. Phys.* **98**, 7029 (1993).
- ¹⁵C. E. Smith, R. A. King, and T. D. Crawford, *J. Chem. Phys.* **122**, 054110 (2005).
- ¹⁶K. Andersson, P.-Å. Malmqvist, B. O. Roos, A. J. Sadlej, and K. Wolinski, *J. Phys. Chem.* **94**, 5483 (1990).
- ¹⁷K. Andersson, P.-Å. Malmqvist, and B. O. Roos, *J. Chem. Phys.* **96**, 1218 (1992).
- ¹⁸B. Roos, M. Fülcher, P.-Å. Malmqvist, M. Merchán, and L. Serrano-Andrés, in *Quantum Mechanical Electronic Structure Calculations with Chemical Accuracy*, edited by S. Langhoff (Kluwer Academic, Dordrecht, 1995), pp. 357–438.
- ¹⁹T. D. Crawford and H. F. Schaefer, in *Reviews in Computational Chemistry*, edited by K. B. Lipkowitz and D. B. Boyd (VCH, New York, 2000), Vol. 14, Chap. 2, pp. 33–136.
- ²⁰C. D. Sherrill and H. F. Schaefer, *Adv. Quantum Chem.* **34**, 143 (1999).
- ²¹R. G. Parr and W. Yang, *Density-Functional Theory of Atoms and Molecules* (Oxford University, New York, 1989).
- ²²M. E. Casida, in *Recent Advances in Density Functional Methods*, edited by D. P. Chong (World Scientific, Singapore, 1995), Vol. 1.
- ²³R. Bauernschmitt and R. Ahlrichs, *Chem. Phys. Lett.* **256**, 454 (1996).
- ²⁴T. H. Dunning, *J. Chem. Phys.* **90**, 1007 (1989).
- ²⁵R. A. Kendall, T. H. Dunning, and R. J. Harrison, *J. Chem. Phys.* **96**, 6796 (1992).
- ²⁶T. W. Robinson, D. P. Schofield, and H. G. Kjaergaard, *J. Chem. Phys.* **118**, 7226 (2003).
- ²⁷K. Raghavachari, G. W. Trucks, J. A. Pople, and M. Head-Gordon, *Chem. Phys. Lett.* **157**, 479 (1989).
- ²⁸R. J. Bartlett, J. D. Watts, S. A. Kucharski, and J. Noga, *Chem. Phys. Lett.* **165**, 513 (1990); **167**, 609 (1990).
- ²⁹A. D. Becke, *J. Chem. Phys.* **98**, 5648 (1993).
- ³⁰C. Lee, W. Yang, and R. G. Parr, *Phys. Rev. B* **37**, 785 (1988).
- ³¹J. Gauss, W. J. Lauderdale, J. F. Stanton, J. D. Watts, and R. J. Bartlett, *Chem. Phys. Lett.* **182**, 207 (1991).
- ³²J. Gauss, J. F. Stanton, and R. J. Bartlett, *J. Chem. Phys.* **95**, 2623 (1991).
- ³³J. F. Stanton and J. Gauss, *J. Chem. Phys.* **99**, 8840 (1993).
- ³⁴T. D. Crawford, C. D. Sherrill, E. F. Valeev *et al.*, *PSI 3.2*, 2003.
- ³⁵J. F. Stanton, J. Gauss, J. D. Watts, W. J. Lauderdale, and R. J. Bartlett, *ACES II*, 1993. The package also contains modified versions of the *MOL-ECULE* Gaussian integral program of J. Almlöf and P. R. Taylor, the *ABACUS* integral derivative program written by T. U. Helgaker, H. J. Aa. Jensen, P. Jørgensen, and P. R. Taylor, and the *PROPS* property evaluation integral code of P. R. Taylor.
- ³⁶R. D. Amos, A. Bernhardsson *et al.*, *MOLPRO*, a package of *ab initio* programs designed by H. J. Werner and P. J. Knowles, Version 2002.6, 2002.
- ³⁷R. Ahlrichs, M. Bärnd, H.-P. Baron *et al.*, *TURBOMOLE v5.6*, 2002.
- ³⁸S. Du, J. S. Francisco, G. K. Schenter, T. D. Iordanov, B. C. Garrett, M. Dupuis, and J. Li, *J. Chem. Phys.* **124**, 224318 (2006).
- ³⁹H. G. Kjaergaard, *J. Phys. Chem. A* **106**, 2979 (2002).

⁴⁰H. G. Kjaergaard, T. W. Robinson, D. L. Howard, J. S. Daniel, J. A. Headrick, and V. Vaida, *J. Phys. Chem. A* **107**, 10680 (2003).

⁴¹J. R. Roscioli, E. G. Diken, M. A. Johnson, S. Horvath, and A. B. McCoy, *J. Phys. Chem. A* **110**, 4943 (2006).

⁴²T. J. Lee and P. R. Taylor, *Int. J. Quantum Chem., Quantum Chem. Symp.* **23**, 199 (1989).

⁴³J. Gillis, A. Goldman, G. Stark, and C. Rinsland, *J. Quant. Spectrosc. Radiat. Transf.* **68**, 225 (2000).